One-Step 18F Labeling of Non-Peptidic Bivalent Integrin αvβ3 Antagonist for Cancer Imaging

Weiwei Wang, Zhiyi Liu, and Zheng Li*

Department of Translational Imaging, The Methodist Hospital Research Institute, Weill Medical College of Cornell University, 6670 Bertner Avenue, Houston, Texas 77030, United States

S Supporting Information

ABSTRACT: A rapid one-step 18F labeling reaction with fluoridealuminum complex, which is based on chelation chemistry, has received a surge of interest for 18F radiolabeling of peptides. In this study, a non-peptidic bivalent integrin αvβ3 antagonist (bivalent-IA) was conjugated with 1,4,7-triazacyclononane-1,4-diiacetic acid (NODA). A novel 18F labeled radiotracer, 18F-bivalent-IA, was developed via one step 18F–AlF/NODA chelation reaction in aqueous phase with high radiochemical yield (65−75%, decay corrected) and good specific activity (750−850 mCi/μmol). The tumor integrin targeting efficiency and in vivo pharmacokinetic profile of 18F-bivalent-IA were evaluated in U-87 MG (integrin positive) and MDA-MB-231 (integrin negative) models by small-animal PET/CT scan followed by a biodistribution study. The PET/CT and ROI results showed high tumor uptake of 18F-bivalent-IA in U-87 MG tumor-bearing mice from 5 to 120 min p.i. with good contrast, and the U-87 MG tumor uptake values (6.35 ± 0.67%ID/g, at 1 h p.i.) were 6 times higher than those of MDA-MB-231 tumor (1.05 ± 0.12%ID/g, at 1 h p.i.) ($P < 0.0001$) which correlated with the integrin αvβ3 expression in tumor tissues confirmed by immunohistochemistry. Co-injection of the 18F-bivalent-IA with 6 nmol (6 μg) of nonradioactive bivalent-IA effectively blocked tumor uptake demonstrating the integrin αvβ3-specificity. In conclusion, the first 18F labeled non-peptidic bivalent integrin αvβ3 targeting radiotracer, 18F-bivalent-IA, was developed and proved to be a highly potent and specific PET radiopharmaceutical for noninvasive imaging of integrin αvβ3, which plays a critical role in tumor angiogenesis and metastasis.
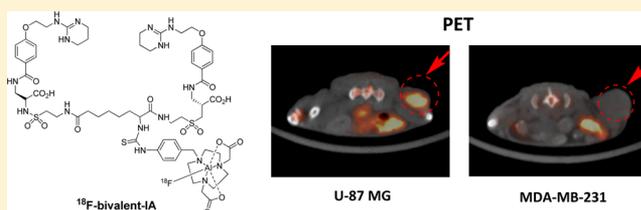
Positron emission tomography (PET) is a clinically used molecular imaging modality to detect cancer and other diseases with high sensitivity.[1] Compared with other positron-emitting isotopes (^{11}C, ^{13}N, ^{15}O, ^{68}Ga, [89]Zr, [124]I), ^{18}F is the most widely used PET radioisotope because of suitable decay, low β[+]-trajectory, and small atomic size.[2,3] Recently, the one-step ^{18}F labeling method with fluoridealuminum complex, which is based on chelation chemistry, has received a surge of interest for peptide radiolabeling.[4−8] In comparison with the classical ^{18}F nucleophilic substitution reaction, which usually involves prosthetic groups with time-consuming multistep radiosynthesis, this new fluorination method is efficient, simple, and straightforward. As a novel chelator with (Al[18]F)[2+] complex, 1,4,7-triazacyclononane-1,4-diiacetic acid (NODA) has excellent binding kinetics, and its Al[18]F complexes are highly stable in vivo.[9−13]

Integrin αvβ3, a receptor for extracellular proteins including vitronectin, fibronectin, and fibrinogen, plays an important role in tumor growth, angiogenesis, local invasiveness, and metastatic potential.[14−16] RGD peptides specifically binding to integrin αvβ3, and their multivalent derivatives have been intensively studied with various radiolabels for noninvasively PET imaging of different cancer types.[6−8,17−20] In comparison with peptide/antibody, small molecules have advantages in developing the imaging moiety owing to their high affinity to target, low immunogenicity, and flexibility in chemical modification. At present, an ^{18}F labeled small-molecule-based

integrin targeting radiotracer has not been reported. Our interest is to develop potent non-peptidic small molecular integrin αvβ3 targeting derivatives as a novel cancer theranostic platform.[21−24] We developed a bivalent-IA compound derived from a small molecule αvβ3 antagonist, 4-[2-(3,4,5,6-tetrahydropyrimidine-2-lamino)-ethyloxy]benzoyl-2-(S)-aminoethyl-sulfonyl-amino-h-alanine (Figure 1, IA) which exhibited subnanomolar range integrin receptor binding affinity (IC$_{50}$ = 0.40 ± 0.11 nM) and potent therapeutic efficacy as a single drug in a tumor xenographic model.[23,24] In this study, we applied this facile and rapid ^{18}F-AlF/NODA chelation method to synthetic small molecule radiolabeling and successfully developed, to the best of our knowledge, the first ^{18}F labeled non-peptidic small molecule integrin αvβ3 targeted radiotracer, ^{18}F-bivalent-IA. Small-animal PET revealed rapid, specific, and prominent uptake of ^{18}F-bivalent-IA in human glioblastoma U-87 MG tumors (high integrin expression) but significantly lower and sporadic uptake in human breast cancer MDA-MB-231 tumors (low integrin expression) which successfully demonstrated the ability of ^{18}F-bivalent-IA to quantitatively visualize integrin αvβ3 expression in vivo. The integrin αvβ3 expression in different tumor types was confirmed by
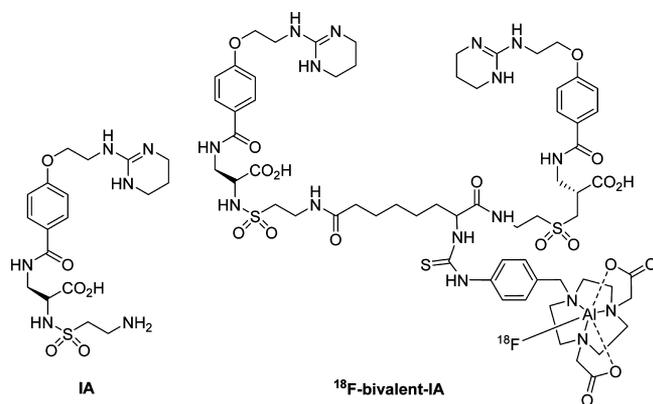
Figure 1. Chemical structures of IA and ^{18}F-bivalent-IA.

immunohistochemical (IHC) staining (see SI, Figure 1S) and was also indicated in the literature.[25,26] With the significant tumor localization, excellent biodistribution, and pharmacokinetic properties, the radiotracer ^{18}F-bivalent-IA used for tumor anti-angiogenic imaging and integrin-targeted therapy evaluation has great potential for future clinical translation.

The precursor bivalent-IA was obtained by a multistep synthesis according to our previously reported procedures.[23] NODA-bivalent-IA was prepared by direct conjugation of bivalent-IA with NCS-MP-NODA (CheMatech, Dijon, France) in 75% yield. The compounds were purified by HPLC and were characterized by MS and NMR (see SI for details). To determine the receptor-binding ability, NODA-bivalent-IA was tested for its ability to competitively inhibit the attachment of

the natural ligand vitronectin to purified human $\alpha_v\beta_3$ (Chemicon International, CA) by enzyme-linked immunosorbent assay (ELISA) (see SI for details). The IC$_{50}$ value of NODA-bivalent-IA was 1.9 ± 0.27 nM (see SI, Figure 3S) which demonstrated that NODA conjugation did not decrease the integrin $\alpha_v\beta_3$ receptor binding affinity.

In the radiolabeling reaction, NODA-bivalent-IA was radio-labeled by incubating with Na^{18}F in 0.5 N NaOAc buffer (pH 4.0) at 100 °C for 15 min (see SI). The labeled product ^{18}F-bivalent-IA (Figure 1, ^{18}F-bivalent-IA) was then directly purified by C18 Classic Cartridge (Waters, Milford, MA). The whole radiosynthesis was accomplished within 25 min with a decay-corrected yield of 65−75% and radiochemical purity of more than 95% ($n = 12$). The specific activity of purified ^{18}F-bivalent-IA was calculated as 750−850 mCi/μmol (27.8−31.6 MBq/μmol). Chemical stability of ^{18}F-bivalent-IA was evaluated by radio-HPLC analysis that revealed no change in the chromatogram after 3 h incubation in mouse serum at 37 °C (see SI, Figure 2S). The radiolabeling and purification procedure of ^{18}F-bivalent-IA, which was a one step reaction with no HPLC purification and no evaporation step, is less laborious and fully scalable for future commercial production.

Glioblastoma is one of the most aggressive tumors, and integrin $\alpha_v\beta_3$ is highly overexpressed in U-87 MG glioblastoma cells.[6,7,17−20] U-87 MG tumor was used to evaluate the in vivo pharmacokinetic profile and tumor targeting property of ^{18}F-bivalent-IA. 60 min dynamic small-animal PET/CT scans followed by static scans at 2 h after tail vein injection of ^{18}F-bivalent-IA were obtained using U-87 MG tumor-bearing mice ($n = 5$ per group). Representative decay-corrected coronal images and regions of interest (ROI) analysis are shown in
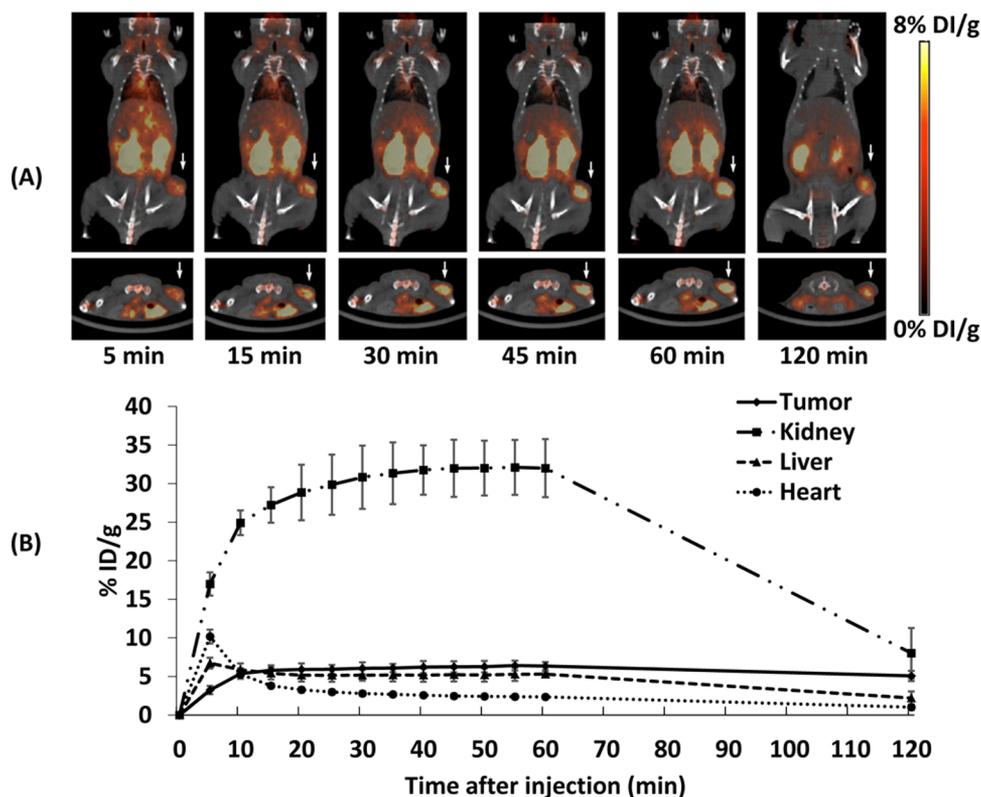

Figure 2. (A) PET/CT images of U-87 MG tumor-bearing mice injected intravenously with approximately 100 μCi of ^{18}F-bivalent-IA. (B) Time−activity curves of tumor and major organs of U-87 MG tumor-bearing mice from 60 min dynamic scans after intravenous injection of ^{18}F-bivalent-IA ($n = 5$). (Tumors are indicated by arrowheads.)

Figure 2. The U-87 MG tumors were clearly visualized with excellent tumor to background contrast for ^{18}F-bivalent-IA as early as 5 min post injection. Compared with normal tissue, quantification of tumor-to-muscle ratios show that, for the U-87 MG tumor, tumor uptake values were over 30 times higher than those of the muscle at 1 h p.i (Figure 3E). From the ROI
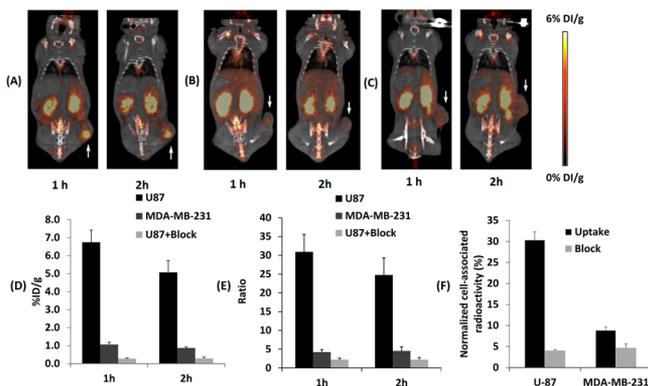

Figure 3. (A) PET/CT images of U-87 MG tumor-bearing mice injected intravenously with ^{18}F-bivalent-IA, and (B) PET/CT images of U-87 MG tumor-bearing mice injected intravenously with ^{18}F-bivalent-IA and 6 nmol (6 μg) of bivalent-IA. (C) PET/CT images of MDA-MB-231 breast tumor-bearing mice injected intravenously with ^{18}F-bivalent-IA. (Tumors are indicated by arrowheads.) (D) Quantitative analysis of small-animal PET/CT images. Comparison of decay-corrected ROI analysis of ^{18}F-bivalent-IA (U-87 MG tumor-bearing mice) ($n = 5$), ^{18}F-bivalent-IA (MDA-MB-231 breast tumor-bearing mice) ($n = 3$), and ^{18}F-bivalent-IA coinjected with 6 nmol (6 μg) of bivalent-IA (U-87 MG tumor-bearing mice) ($n = 4$) in tumor. (E) Comparison of tumor-to-muscle uptake ratios after injection of ^{18}F-bivalent-IA (U-87 MG tumor-bearing mice) ($n = 5$), ^{18}F-bivalent-IA (MDA-MB-231 breast tumor-bearing mice) ($n = 3$), and ^{18}F-bivalent-IA coinjected with 6 nmol (6 μg) of bivalent-IA (U-87 MG tumor-bearing mice) ($n = 4$). (F) Cell uptake and competition assay. Binding of ^{18}F-bivalent-IA to U-87 MG and MDA-MB-231 cells with varying levels of integrin $\alpha_v\beta_3$.

analysis displayed in Figure 2B, in the first 15 min after tail vein injection, radioactivity rapidly accumulated in the tumor (5.80 ± 0.65%ID/g) and was maintained throughout the entire scan process (5.07 ± 0.66%ID/g, at 2 h p.i.). The tumor uptake peaked (6.42 ± 6.3%ID/g) at 55 min p.i. In contrast, heart uptake peaked (10.18 ± 0.9%ID/g) at 5 min p.i. but decreased to 2.68 ± 0.29%ID/g at 20 min p.i.. High radioactivity accumulated in the kidneys at 60 min p.i. (32.00 ± 3.77%ID/g) and rapidly decreased at 2 h post injection (8.02 ± 3.26%ID/g, at 2 h p.i.) demonstrating fast renal excretion. Low levels of liver uptake were also observed at all time points. The bone uptake was measured as 0.34 ± 0.05%ID/g at 1 h p.i. and 0.20 ± 0.07%ID/g at 2 h p.i., respectively, indicating good in vivo stability of the ^{18}F-bivalent-IA.

To further demonstrate ^{18}F-bivalent-IA for in vivo integrin $\alpha_v\beta_3$ receptor expression imaging, we also evaluated it using human breast MDA-MB-231 tumors with low integrin expression as a negative comparison.[25] The PET/CT images of MDA-MB-231 breast tumor bearing mice of 1 h and 2 h postinjection are shown in Figure 3C. The MDA-MB-231 tumor uptake values were 1.05 ± 0.12 and 0.86 ± 0.06%ID/g at 1 and 2 h p.i. respectively, which were six times lower than those of the U-87 MG tumor (6.35 ± 0.67%ID/g, at 1 h p.i. and 5.07 ± 0.66%ID/g, at 2 h p.i., Figure 3D) ($P < 0.0001$). High integrin $\alpha_v\beta_3$ expression in U-87 MG tumors and low

expression in MDA-MB-231 tumors were confirmed by immunohistochemical (IHC) staining (see SI, Figure 1S). The in vitro cell uptake and blocking study of ^{18}F-bivalent-IA was also performed using U-87 MG and MDA-MB-231 cell lines (Figure 3F; for detailed procedures see SI). The radiotracer uptake levels revealed that ^{18}F-bivalent-IA represented a 4-fold-higher avidity with U-87 MG cells over MDA-MB-231 cells in vitro ($P < 0.0001$). The cell uptake was successfully blocked by coincubation with unlabeled bivalent-IA in U-87 MG cells which demonstrated specific binding to cell integrin $\alpha_v\beta_3$ receptor.

The integrin $\alpha_v\beta_3$ specificity of ^{18}F-bivalent-IA was confirmed by the blocking experiments in vivo. The PET/CT images at 1 and 2 h p.i. of U-87 MG tumor-bearing nude mice coinjected with ^{18}F-bivalent-IA and 6 nmol (6 μg) unlabeled bivalent-IA are shown in Figure 3B. The U-87 MG tumor uptake was effectively blocked to the background level. The ROI analysis (Figure 3D) showed that the uptake values were very low as 0.27 ± 0.03 and 0.28 ± 0.07%ID/g at 1 and 2 h p.i., respectively, in the blocking study.

Biodistribution studies were performed at 3 h postinjection after the microPET/CT scans for all imaging studies. Tumors and major organs were harvested, weighed, and the radio-activity was counted (Figure 4). The results demonstrated
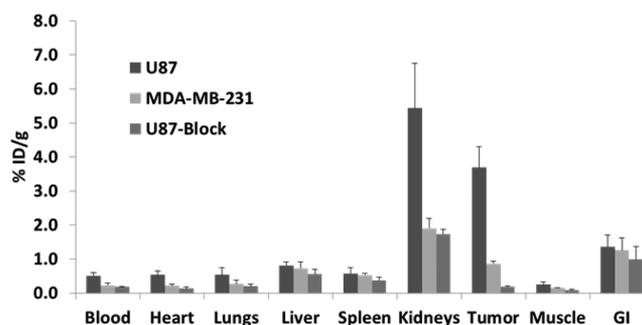

Figure 4. Biodistribution at 3 h postinjection ^{18}F-NODA-bivalent-IA (U-87 MG tumor-bearing mice) ($n = 5$), ^{18}F-NODA-bivalent-IA (MDA-MB-231 breast tumor-bearing mice) ($n = 3$), and ^{18}F-NODA-bivalent-IA coinjected with blocking dose of bivalent-IA (U-87 MG tumor-bearing mice) ($n = 4$).

excellent tumor uptake of ^{18}F-bivalent-IA in U-87 MG tumor-bearing mice (3.69 ± 0.62%ID/g), which was more than 4 times higher than that of MDA-MB-231 tumor-bearing mice (0.86 ± 0.07%ID/g) ($P < 0.001$). Competition performed with ^{18}F-bivalent-IA and a block dose (6 nmol, 6 μg) of nonradioactive bivalent-IA decreased tumor uptake to 0.18 ± 0.03%ID/g, which was approximately 20 times lower than mice imaged without cold compound ($P < 0.0001$). All biodistribution results in imaging and blocking study in different animal models had good correlation with semiquantitative ROI analysis of PET imaging studies.

In this study, we have successfully developed the first ^{18}F labeled non-peptidic bivalent integrin $\alpha_v\beta_3$ targeting radiotracer using a one step ^{18}F-AlF/NODA chelation reaction. The results demonstrate that ^{18}F-bivalent-IA is a highly potent and specific PET radiopharmaceutical to noninvasively image integrin $\alpha_v\beta_3$ in murine xenograft tumor models. Studies have shown the level of $\alpha_v\beta_3$ expression varies among individual cancer patients and high integrin $\alpha_v\beta_3$ expression has been correlated with disease progression and poor survival.[26−28] This new radio-tracer, which can quantitatively visualize tumor integrin

expression by PET, has great potential for accurate cancer staging, patient selection for anti-integrin treatments, and therapy efficacy monitoring. Specially, ^{18}F radiopharmaceutical is usually a time-consuming process with custom synthesis; the labeling procedures for the small molecule compound in this study is suitable to formulate into a lyophilized kit for ^{18}F radiolabeling in the future. Further evaluation of safety and toxicology of ^{18}F-bivalent-IA is ongoing.

■ ASSOCIATED CONTENT

Ⓢ Supporting Information

Detailed methods of chemistry and radiolabeling of ^{18}F-bivalent-IA, ELISA, cell uptake and blocking assay, small-animal PET imaging, biodistribution study, tumor tissue immunohistochemistry, and mouse serum stability study. This material is available free of charge via the Internet at http://pubs.acs.org.

■ AUTHOR INFORMATION

Corresponding Author

*E-mail: ZLi@houstonmethodist.org.

Notes

The authors declare no competing financial interest.

■ ACKNOWLEDGMENTS

■ REFERENCES

(1) Ametamey, S. M., Honer, M., and Schubiger, P. A. (2008) Molecular imaging with PET. *Chem. Rev. 108*, 1501−1516.

(2) Miller, P. W., Long, N. J., Vilar, R., and Gee, A. D. (2008) Synthesis of ^{11}C, ^{18}F, ^{15}O, and ^{13}N radiolabels for positron emission tomography. *Angew. Chem., Int. Ed. 47*, 8998−9033.

(3) Cai, L., Lu, S., and Pike, V. W. (2008) Chemistry with [^{18}F] fluoride ion. *Eur. J. Org. Chem.*, 2853−2873.

(4) McBride, W. J., Sharkey, R. M., Karacay, H., D'Souza, C. A., Rossi, E. A., Laverman, P., Chang, C.-H., Boerman, O. C., and Goldenberg, D. M. (2009) A novel method of ^{18}F radiolabeling for PET. *J. Nucl. Med. 50*, 991−998.

(5) McBride, W. J., D'Souza, C. A., Sharkey, R. M., Karacay, H., Rossi, E. A., Chang, C.-H., and Goldenberg, D. M. (2010) Improved ^{18}F labeling of peptides with a fluoride-aluminum-chelate complex. *Bioconjugate Chem. 21*, 1331−1340.

(6) Liu, S., Liu, H., Jiang, H., Xu, Y., Zhang, H., and Cheng, Z. (2011) One-step radiosynthesis of ^{18}F-AlF-NOTA-RGD$_2$ for tumor angiogenesis PET imaging. *Eur. J. Nucl. Med. Mol. Imaging 38*, 1732−1741.

(7) Lang, L., Li, W., Guo, N., Ma, Y., Zhu, L., Kiesewetter, D. O., Shen, B., Niu, G., and Chen, X. (2011) Comparison study of [^{18}F]FAl-NOTA-PRGD2, [^{18}F]FPPRGD2, and [^{68}Ga]Ga-NOTA-PRGD2 for PET imaging of U87MG tumors in mice. *Bioconjugate Chem. 22*, 2415−2422.

(8) Gao, H., Lang, L., Guo, N., Cao, F., Quan, Q., Hu, S., Kiesewetter, D. O., Niu, G., and Chen, X. (2012) PET imaging of angiogenesis after myocardial infarction/reperfusion using a one-step labeled integrin-targeted tracer ^{18}F-AlF-NOTA-PRGD2. *Eur. J. Nucl. Med. Mol. Imaging 39*, 683−692.

(9) Shetty, D., Choi, S. Y., Jeong, J. M., Lee, J. Y., Hoigebazar, L., Lee, Y.-S., Lee, D. S., Chung, J.-K., Lee, M. C., and Chung, Y. K. (2011) Stable aluminium fluoride chelates with triazacyclononane derivatives proved by X-ray crystallography and ^{18}F-labeling study. *Chem. Commun. 47*, 9732−9734.

(10) D'Souza, C. A., McBride, W. J., Sharkey, R. M., Todaro, L. J., and Goldenberg, D. M. (2011) High-yielding aqueous ^{18}F-labeling of peptides via Al[18]F chelation. *Bioconjugate Chem. 22*, 1793−1803.

(11) McBride, W. J., D'Souza, C. A., Karacay, H., Sharkey, R. M., and Goldenberg, D. M. (2012) New lyophilized kit for rapid radio-fluorination of peptides. *Bioconjugate Chem. 23*, 538−547.

(12) Hoigebazar, L., Jeong, J. M., Lee, J.-Y., Shetty, D., Yang, B. Y., Lee, Y.-S., Lee, D. S., Chung, J.-K., and Lee, M. C. (2012) Syntheses of 2-nitroimidazole derivatives conjugated with 1,4,7-triazacyclononane-N,N'-diacetic acid labeled with F-18 using an aluminum complex method for hypoxia imaging. *J. Med. Chem. 55*, 3155−3162.

(13) Lütje, S., Franssen, G. M., Sharkey, R. M., Laverman, P., Rossi, E. A., Goldenberg, D. M., Oyen, W. J. G., Boerman, O. C., and McBride, W. J. (2014) Anti-CEA antibody fragments labeled with [^{18}F]AlF for PET imaging of CEA-Expressing Tumors. *Bioconjugate Chem. 25*, 335−341.

(14) Brooks, P. C., Clark, R. A., and Cheresh, D. A. (1994) Requirement of vascular integrin alpha v beta 3 for angiogenesis. *Science 264*, 569−571.

(15) Hood, J. D., Bednarski, M., Frausto, R., Guccione, S., Reisfeld, R. A., Xiang, R., and Cheresh, D. A. (2002) Tumor regression by targeted gene delivery to the neovasculature. *Science 296*, 2404−2407.

(16) Takagi, J., and Springer, T. A. (2002) Integrin activation and structural rearrangement. *Immunol. Rev. 186*, 141−163.

(17) Liu, Z., Yan, Y., Liu, S., Wang, F., and Chen, X. (2009) ^{18}F, ^{64}Cu, and ^{68}Ga labeled RGD-bombesin heterodimeric peptides for PET imaging of breast cancer. *Bioconjugate Chem. 20*, 1016−1025.

(18) Yang, Y., Ji, S., and Liu, S. (2014) Impact of multiple negative charges on blood clearance and biodistribution characteristics of [99]mTc-labeled dimeric cyclic RGD peptides. *Bioconjugate Chem. 25*, 1720−1729.

(19) Delbaldo, C., Raymond, E., Vera, K., Hammershaimb, L., Kaucic, K., Lozahic, S., Marty, M., and Faivre, S. (2008) Phase I and pharmacokinetic study of etaracizumab (Abegrin), a humanized monoclonal antibody against alphavbeta3 integrin receptor, in patients with advanced solid tumors. *Invest. New Drugs 26*, 35−43.

(20) Schottelius, M., Laufer, B., Kessler, H., and Wester, H. (2009) Ligands for mapping $\alpha_v\beta_3$ integrin expression in vivo. *Acc. Chem. Res. 42*, 969−980.

(21) Burnett, C. A., Xie, J., Quijano, J., Shen, Z., Hunter, F., Bur, M., Li, K. C., and Danthi, S. N. (2005) Synthesis, in vitro, and in vivo characterization of an integrin alpha(v)beta(3)-targeted molecular probe for optical imaging of tumor. *Bioorg. Med. Chem. 13*, 3763−3771.

(22) Xie, J., Shen, Z., Li, K. C., and Danthi, N. (2007) Tumor angiogenic endothelial cell targeting by a novel integrin-targeted nanoparticle. *Int. J. Nanomed. 2*, 479−485.

(23) Li, F., Liu, J., Jas, G. S., Zhang, J., Qin, G., Xing, J., Cotes, C., Zhao, H., Wang, X., Diaz, L. A., Shi, Z.-Z., Lee, D. Y., Li, K. C. P., and Li, Z. (2010) Synthesis and evaluation of a near-infrared fluorescent non-peptidic bivalent integrin $\alpha_v\beta_3$ antagonist for cancer imaging. *Bioconjugate Chem. 21*, 270−278.

(24) Kim, Y.-S., Li, F., Kong, R., Bai, Y., Li, K. C. P., Fan, Y., O'Neill, B. E., and Li, Z. (2013) Multivalency of non-peptide integrin $\alpha_v\beta_3$ antagonist slows tumor growth. *Mol. Pharmaceutics 10*, 3603−3611.

(25) Taherian, A., Li, X., Liu, Y., and Haas, T. A. (2011) Differences in integrin expression and signaling within human breast cancer cells. *BMC Cancer 11*, 293−307.

(26) Schnell, O., Krebs, B., Wagner, E., Romagna, A., Beer, A. J., Grau, S. J., Thon, N., Goetz, C., Kretzschmar, H. A., Tonn, J., and Goldbrunner, R. H. (2008) Expression of integrin $\alpha_v\beta_3$ in gliomas correlates with tumor grade and is not restricted to tumor vasculature. *Brain Pathol. 18*, 378−386.

(27) Sato, T., Konishi, K., Kimura, H., Maeda, K., Yabushita, K., Tsuji, M., and Miwa, A. (2001) Vascular integrin beta 3 and its relation to pulmonary metastasis of colorectal carcinoma. *Anticancer Res. 21*, 643−647.

(28) Vonlaufen, A., Wiedle, G., Borisch, B., Birrer, S., Luder, P., and Imhof, B. A. (2001) Integrin alpha(v)beta(3) expression in colon carcinoma correlates with survival. *Mod. Pathol. 14*, 1126−1132.